

Effect of soil and water conservation measures on regime-based suspended sediment load during floods

Jinfei Hu^{a,c}, Guangju Zhao^{a,b,*}, Xingmin Mu^{a,b,*}, Georg Hörmann^d, Peng Tian^e, Peng Gao^{a,b},
Wenyi Sun^{a,b}

^a State Key Laboratory of Soil Erosion and Dryland Farming on the Loess Plateau, Institute of Soil and Water Conservation, Chinese Academy of Sciences and Ministry of Water Resources, Xinong Road 26, Yangling, 712100, Shaanxi Province, China

^b State Key Laboratory of Soil Erosion and Dryland Farming on the Loess Plateau, Northwest A&F University, 26 Xinong Road, Yangling, 712100, Shaanxi Province, China

^c University of Chinese Academy of Sciences, Beijing, 100049, China

^d Christian-Albrechts-Universität Kiel, Ecology Centre, Department of Hydrology and Water Resources Management, Olshausen str. 40, D-24098, Kiel, Germany

^e College of Resources and Environment, Northwest A&F University, 26 Xinong Road, Yangling, 712100, Shaanxi Province, China

ARTICLE INFO

Keywords:

Event scale
Flood regime
Hyperconcentrated flow
Support vector machines
Sediment yield

ABSTRACT

Understanding the changes in runoff-sediment relationships is a great help for implementing soil and water conservation measures, particularly in regions with severe erosion. We selected a typical coarse sandy catchment on the Loess Plateau to investigate the changes of the runoff-sediment relationships with a data set of 62 years. A change point occurred in 1979, dividing the runoff and sediment load series into a baseline period (1954–1979) and a changing period (1980–2015). A total of 342 flood events were classified into three regimes using hierarchical clustering method. Regime A (162 events) was characterized by the shortest duration, lowest flood crest, and the least flow depth. Regime B (165 events) was characterized by a medium runoff depth, medium flow variability, and medium duration. Regime C merely include fifteen events with longest flood duration, the highest runoff depth, and the largest peak discharge. The sediment yield of flood regime A, B, and C accounted 14.2 % (1.09×10^8 t), 51.8 % (3.99×10^8 t), and 34.0 % (2.62×10^8 t) of the total sediment yield, respectively. The Support vector machines method was applied to established models to predict event sediment yield. It is demonstrated that the performance of models are good for different flood regimes.

1. Introduction

Soil erosion is widespread and a major environmental threat to ecological and social economic systems in different parts of the world. It has direct impact such as the degradation of soil physical, chemical and biological properties as well as soil nutrient loss (Lal, 2003), land productivity decline (Pimentel, 2006). Soil erosion also brings about indirect influences, such as reservoir sedimentation, riverbed rise, channel silting and exacerbate risks of floods and droughts (Mullan, 2013). For example, the flood of 1987 arose from soil erosion on the South Downs in East Sussex, UK, resulting in an economic loss of about €957,000 (Robinson & Blackman, 1990). Therefore, the direct and indirect impacts will pose a major threat to sustainable socio-economic development and water security.

Factors such as climate, topography, vegetation, natural disturbances and artificial disturbances all have influence on both

processes of soil erosion and the subsequent sediment delivery (Verstraeten, Prosser, & Fogarty, 2007; Zheng, Qin, Yang, & Cai, 2013). Extensive research has been conducted centered on the trend change of runoff and sediment load in many basins (Buendia et al., 2016; Wang et al., 2007). Besides the change of runoff and sediment load, the runoff-sediment relationship is also a key element to determine sediment dynamics. In recent decades, changes in the relationship between runoff and sediment yield have received increasing attention (Gao, Ma, & Fu, 2016; Zheng, Yang, Qi, Sun, & Cai, 2012). Understanding the mechanisms of the runoff-sediment relationship change is crucial to determining the influencing factors of erosion and sediment delivery processes and developing strategic plans for soil erosion control measures.

Sediment yield describes the amount of eroded soil delivered by water to specified sites in a landscape or river system at a certain timescale (Lu, Moran, & Sivapalan, 2005; Verstraeten & Poesen, 2001;

* Corresponding authors at: State Key Laboratory of Soil Erosion and Dryland Farming on the Loess Plateau, Chinese Academy of Sciences and Ministry of Water Resources, 26 Xinong Road, Yangling, 712100, Shaanxi Province, China.

E-mail addresses: gjzhao@ms.iswc.ac.cn (G. Zhao), xmmu@ms.iswc.ac.cn (X. Mu).

<https://doi.org/10.1016/j.scs.2020.102044>

Received 7 January 2019; Received in revised form 9 October 2019; Accepted 7 January 2020

Available online 14 January 2020

2210-6707/ © 2020 Elsevier Ltd. All rights reserved.

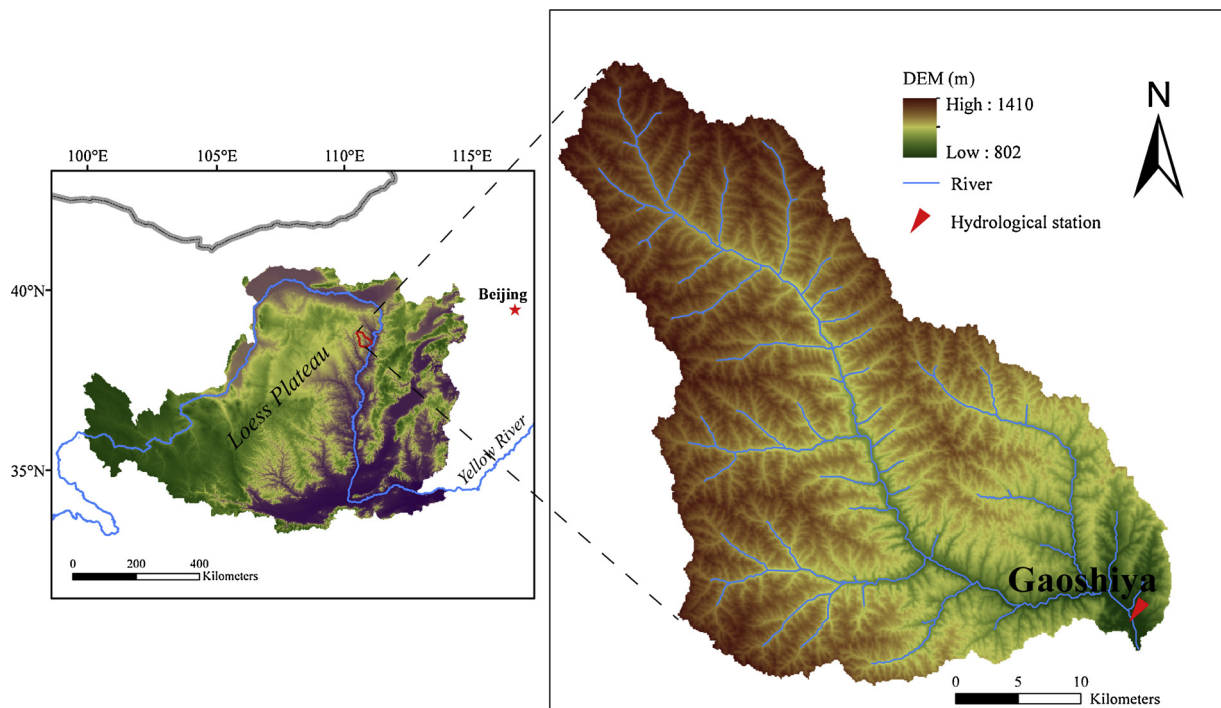


Fig. 1. Location of the study area.

Wasson, 1994). Surface runoff is the basic driving force of soil erosion and the transport medium of sediment. Sediment yield is the end result of erosion and deposition processes and is thus dependent on all factors that influence runoff and erosion processes, including climate, vegetation, topography, land use, and soil physical properties (Buendia et al., 2016; El Kateb, Zhang, Zhang, & Mosandl, 2013; Gain & Wada, 2014; Simonneaux et al., 2015; Walling, 2006). Human activities such as afforestation/deforestation, terraces and check dams have altered the underlying surface condition therein, leading to considerable changes in soil erosion, as well as the relationship between runoff and sediment (Lørup, Refsgaard, & Mazvimavi, 1998). Therefore, identifying the change of runoff-sediment relationships will elucidate the mechanisms of runoff and sediment generation more clearly. This might be helpful to improve the accuracy of soil erosion predictions and optimize the design and layout of soil and water conservation measures (Fang, Cai, Chen, & Li, 2008; Parsons & Stone, 2006; Ran, Su, Li, & He, 2012).

Most previous investigations have been conducted at plot and hillslope scale by measuring the impact of different treatments on runoff and erosion to evaluate the effectiveness of water and soil conservation measures (Bautista, Mayor, Bourakhouadar, & Bellot, 2007; Boix-Fayos et al., 2006; Zheng, Cai, & Chen, 2007). Results obtained from plot and hillslope scale may increase the understanding of the impact of soil conservation measures on erosion and sediment yield (Walling, 1999). However, in most cases, it rarely reflects how a catchment responds to management measures. Only a small fraction of the detached and transported soil material reaches the catchment outlet (Chaplot & Poesen, 2012). Thus, the sediment yield from a catchment is actually much lower than that estimated based on plot and hillslope experiments. That is, plot and hillslope scale studies only take on-site soil detachment into account, while ignoring the off-site effect of sediment transport. Thus, these results are difficult to apply at the catchment and region scale. Additionally, recent research has investigated the influence of different rainfall regimes and underlying surfaces variation on erosion and runoff-sediment relationships (Fang et al., 2012; Peng & Wang, 2012). The analysis of runoff-sediment relationships under different rainfall patterns can improve the reliability of soil erosion predictions and soil erosion control techniques (Parsons & Stone, 2006; Ran et al., 2012). However, few studies pay attention to the changes in

runoff-sediment relationships of different runoff regimes under the impact of water and soil conservation measures. Therefore, further event-based investigation toward a comprehensive assessment of runoff-sediment relationships must be performed under different hydrologic regimes as well as different water and soil conservation measures.

The Loess Plateau suffered from severe soil erosion caused by highly erodible loess soils, intensive rainstorms, steep landscape and poor vegetation cover (Zhang & Liu, 2005). Severe soil erosion harms regional ecosystems and social economy seriously, resulting in land degradation and socioeconomic problems (Mu, Zhang, McVicar, Chille, & Gao, 2007). Therefore, soil and water conservation measures have been enhanced and ecological projects have been implemented during the past decades (Li et al., 2017; Wang et al., 2007). These measures have greatly altered the soil surface properties of the catchment, resulting in significant changes of runoff and sediment load. Consequently, analyzing the dynamics of the runoff-sediment relationship before and after the watershed management is essential to understand the process of runoff and sediment regulation and to develop effective soil erosion control strategies (Zhao et al., 2017). Therefore, the main objectives of this study are: (1) to identify the dominant runoff variables that have a major impact on sediment yield; (2) to explore the effects of soil and water conservation measures on runoff-sediment relationships; (3) to describe the relationship between the sediment yield and effective runoff-related variables.

2. Study area

The Gushanchuan catchment (N 39°00'00"-39°27'36", E 110°32'24"-111°05'24") covers an area of 1,272 km² and is located in the middle reaches of the Yellow River. The soil types in this catchment include loess soil and chestnut soil, with loess soil as the main type. It is one of the first-order tributaries of the Yellow River with a main river length of 79.4 km and average channel gradient of 5.4%. The river originates from Inner Mongolia and eventually flows into the Yellow River. The drainage area gauged at the Gaoshiya hydrological station is 1263 km² (Fig. 1). The catchment is characterized by a typical arid and semi-arid continental monsoon climate. The annual average

precipitation is calculated as approximately 410 mm based on Thiessen polygon method. Precipitation has significant intra-annual and inter-annual variability and most of the annual precipitation is concentrated between June and September, mainly as short-duration, high-intensity rainstorms. The hyper-concentrated sediment flow occurred frequently in the rainy season, with a maximum suspended sediment concentration higher than 1000 kg/m³ (Yang et al., 2010; Yellow River Conservancy Committee, 1954). The average annual runoff and sediment load at the gauging station is 6.47 × 10⁷ m³ (51 mm/a) and 1.62 × 10⁷ t (12,711 t/km²/a), respectively (Yellow River Conservancy Committee, 1954).

3. Material and methods

3.1. Data

The Gaoshiya gauging station was established in 1954 to collect the runoff and suspended sediment concentration data. The maintainance of the gauging station as well as data collection was conducted by the Yellow River Conservancy Commission (YRCC) of the Ministry of Water Resources of People's Republic of China (PRC). The all measured runoff and suspended sediment concentration data were recorded in the Hydrological Yearbook of the Yellow River (Yellow River Conservancy Committee, 1954). A total of 342 flood events were observed at the Gaoshiya hydrological station within 1954–2015. The water level was measured by an automatic recorder and the discharge was calculated with a calibrated water stage/discharge curve. A bottle type sediment sampler was used to collect the sediment flow during each flood event. The suspended sediment concentration was measured with the gravimetric method in the laboratory (Fang et al., 2012; Tian, Zhai, Zhao, & Mu, 2016). During flood events, the sampling interval of sediment flow was shortened to periods between 6 and 12 min during flood peaks and extended to 4–6 h after the flood release. The sediment yield of single flood events was calculated using runoff, suspended sediment concentration, and the sampling interval.

3.2. Methodologies

3.2.1. Flood events indices

The runoff-related variables were used to generalize the individual flood hydrographs, whereas the sediment-relevant variables were selected to characterize the event-based sediment delivery. For a specific flood event, the time interval for the hydrological observations is assumed as Δt, instantaneous discharge and mean suspended sediment concentration (SSC) are Q_t and S_t, respectively, and the controlled area of the gauging station is A. According to the definition presented in previous studies (Zhang, Li, Wang, & Xiao, 2016; Zhao et al., 2017), the runoff and sediment factors of flood event were expressed as follows.

The runoff depth (H) of the flood event is calculated as follows:

$$H(t_1, t_2) = \frac{\int_{t_1}^{t_2} Q_t dt}{A} = \frac{\sum Q_t \Delta t}{A} \quad (1)$$

The sediment yield (SY) for a flood event within the interval (t₁, t₂) can be calculated as:

$$SY(t_1, t_2) = \frac{\int_{t_1}^{t_2} S_t Q_t dt}{A} = \frac{\sum S_t Q_t \Delta t}{A} \quad (2)$$

The flow variability is defined as the ratio of flood peak discharge (Q_p) to mean discharge (Q_m), which can be estimated as:

$$FV = \frac{Q_p}{Q_m} \quad (3)$$

The SSC variability is defined as the ratio of maximum SSC (S_{max}) to SSC, which can be estimated as:

$$SCV = \frac{S_{max}}{SSC} \quad (4)$$

We assessed the event-based runoff and sediment yield characteristics by using above defined hydrological variables.

3.2.2. Identification of baseline and changing periods

To investigate the impact of human activities on hydrological variables, the whole study period would be divided into two or more stages in most studies (Shi & Wang, 2015; Zhao et al., 2018). The first period is the baseline period, when relatively limited or even no human activities occurred. And the second period represents the changing period, when the catchment experienced intensive human activities. The abrupt change point method is often employed to identify the baseline period and changing period. Numerous methods available for identifying the abrupt change point, including the sequential cluster analysis, Pettitt test, the sequential Mann-Kendall test, double mass curve and accumulative anomaly method et al. (Wu, Miao, Zhang, Yang, & Duan, 2017). Yue, Mu, Zhao, Shao, and Gao (2014) have detected the hydrological sequence change point in Gushanchuan catchment using the sequential cluster analysis method. Thus, we used the results directly in present study. According to the abrupt breakpoint detected, the whole time series could be divided into two periods: the baseline period (1971–1979) and the changing period (1980–2015).

3.2.3. Clustering analysis

A clustering approach was applied to classify numerous flood events into different groups for further investigation. Clustering analysis has been widely used to classify objects based on their resemblance in scientific fields (Fang et al., 2012; Peng & Wang, 2012). In this study, the hierarchical clustering method was employed to classify the corresponding flood events by trial and error. The number of clusters are calculated by means of statistical analysis. Discriminant analysis was applied to determine the optimal clusters by Fisher's discriminant function. The Fisher's discriminant functions were as follows:

$$G_1 = -0.021H + 0.02T + 0.014Q_p - 45.515 \quad (5)$$

$$G_2 = -0.381H + 0.009T + 0.004Q_p - 5.13 \quad (6)$$

$$G_3 = -0.542H + 0.016T + 0.007Q_p - 14.768 \quad (7)$$

Where G_k (k = 1, 2, 3) is the classification score for group k.

In the current study, Tukey's test was applied for multiple comparisons in order to compare the various hydrological variables in the baseline period and changing period under different flood regimes.

3.2.4. Support vector machines

Support Vector Machines (SVM) are a widely used machine learning methods developed in recent years on the basis of the foundations of Statistical Learning Theory. Libsvm is one of the most frequently used libraries in various research field (Chang & Lin, 2011). Thus, in current study, the Libsvm program was selected to establish SVM models. The whole dataset is randomly split into the training set and test set. Then the training set is used to build models using the support vector machine (SVM), the test set is used to test the corresponding models. In the current study, 75 % of the flood events is used for training and the remaining 25 % for testing.

Root Mean Squared Error (RMSE) is the square root of the mean of the squared errors:

$$RMSE = \sqrt{\frac{1}{n} \sum_{i=1}^n (SY_o - SY_p)^2} \quad (8)$$

Where SY_o denotes the observed sediment yield, SY_p is the predicted sediment yield.

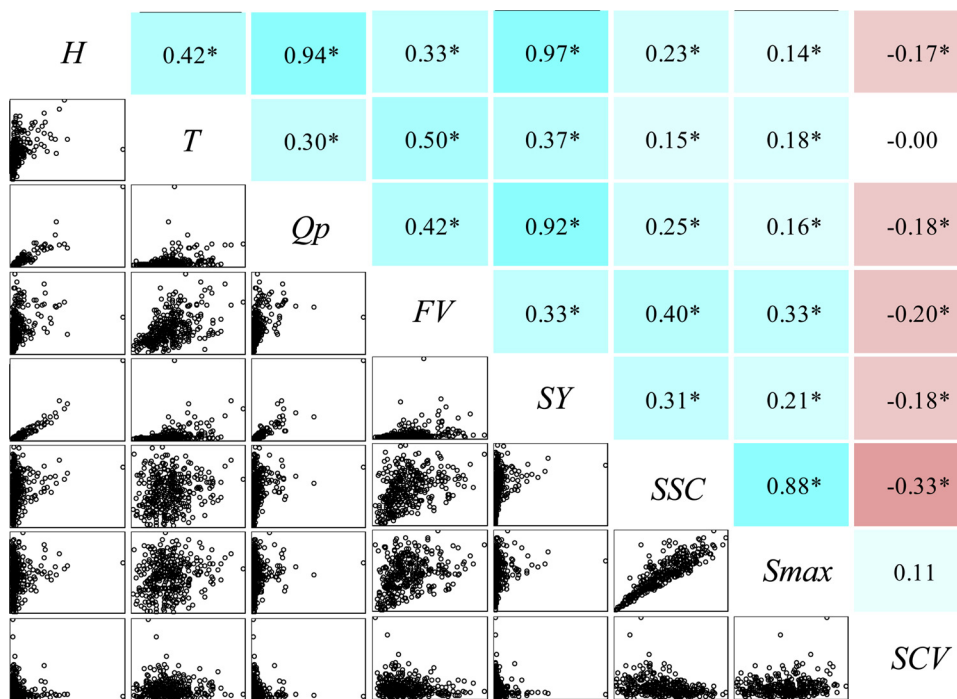


Fig. 2. Correlation analysis among runoff and sediment variables. (Note: *H*, event flood runoff depth; *T*, event flood duration; *Q_p*, event peak discharge; *FV*, flow variability, defined as the ratio of peak discharge to mean discharge; *SY*, event sediment yield; *SSC*, event average suspended sediment concentration; *S_{max}*, event maximum suspended sediment concentration; □ significance at the 0.05 level. The same as below.).

4. Results

4.1. Flood events classification

Fig. 2 showed the correlation matrix between hydrologic and sediment variables as well as the correlation coefficients. The *SY* had significant correlations ($p < 0.01$) with runoff variables (*H*, *Q_p*, and *FV*). It is obvious that the correlation between *H* and *SY* was the strongest. Thus, the runoff depth could be considered as the most important variable influencing *SY*. Meanwhile, *Q_p* represented the potential of sediment detachment and delivery, and the variable was also well correlated with *SSC* and *SY*. Hence, the sediment yield was not only determined by the total amount of runoff, but also related to other variables. As well, flood duration (*T*) showed strong relationship with *SY*. It characterized the duration of runoff erosivity effects and sediment delivery process at the event scale. Consequently, three variables including the runoff depth, flood duration and peak discharge were employed as basic indicators to classify the flood events.

Based on the three basic indicators selected above, the hierarchical clustering method was used to classify the flood events. The flood events were then classified into three regimes with significance level at $P < 0.01$ (Table 1). Flood events in Regime A occurred 162 times, and flood Regime B has the highest frequency among these three regimes

Table 1
Statistical features of runoff-related variables under different flood regimes.

Flood regime	Variable	Statistical Description			
		Frequency	Mean	Standard deviation	Variation of coefficient
A	<i>H</i> / mm	162	1.32	1.20	0.91
	<i>T</i> / min	913	242		0.26
	<i>Q_p</i> / m ³ ·s ⁻¹	145.6	143.1		0.98
B	<i>H</i> / mm	165	4.56	4.63	1.02
	<i>T</i> / min	1695	396		0.23
	<i>Q_p</i> / m ³ ·s ⁻¹	423.2	447.8		1.06
C	<i>H</i> / mm	15	27.53	7.82	0.28
	<i>T</i> / min	2193	644		0.29
	<i>Q_p</i> / m ³ ·s ⁻¹	2894	882		0.30

with a total of 165 flood events, whereas flood Regime C has 16 events. The mean runoff depth, flood duration, peak discharge, and flood variability increased in the following order: Regime A < Regime B < Regime C. Individually, Regime A was composed of flood events with the least flow depth (1.32 mm), the shortest duration (913 min), the lowest peak discharge (145.6 m³·s⁻¹), and the lowest flood variability (4.6). Regime B was characterized by a moderate runoff depth (4.56 mm), moderate duration (1695 min), moderate peak discharge (423.2 m³·s⁻¹), and moderate flow variability (7.1). Flood events in Regime C have the highest runoff depth (27.53 mm), the longest duration (2193 min), maximum peak discharge (2894 m³·s⁻¹), and highest flow variability (10.9). The summed runoff depths from flood Regimes A, B, and C accounted for 16 % (214.31 mm), 54 % (752.25 mm), and 30 % (412.98 mm) of the total amount, respectively, suggesting that the primary low-frequency runoff-producing events are mainly from Regimes C.

4.2. Changes in hydrological and sediment characteristics

Fig. 3 showed six main indices representing the change of event-scale hydrological variables with different flood regimes in both baseline period and changing period. The runoff and sediment variables (*H*, *Q_p*, *SY*, *S_{max}*, and *SSC*) decreased for all flood regimes during the baseline period compared with those in the changing period. Specially, for Regime A (minor flood events), the *S_{max}* and *SSC* were much lower in changing period than those in baseline period. In addition, the all indices except *T* had significant reduction during the changing period compared to the baseline period for Regime B. With respect to the large flood events (Regime C), the *SY* reduced dramatically during the changing period. For example, the sediment yield ranged from 9848 to 25364 t/km² between 1971 and 1979 and from 5215 to 20292 t/km² between 1980 and 2015 for Regime C. This suggested that soil and water conservation measures had an influence on the mechanism of runoff and sediment delivery for various flood regimes.

Fig. 3f showed that the average sediment yield for flood events of Regime C is the largest, whereas the average sediment yield of Regime A is the least. The average sediment yield produce by flood events of Regime C is significantly higher than that by flood events of Regimes A and B. The contribution of gross sediment yield by each flood regime to

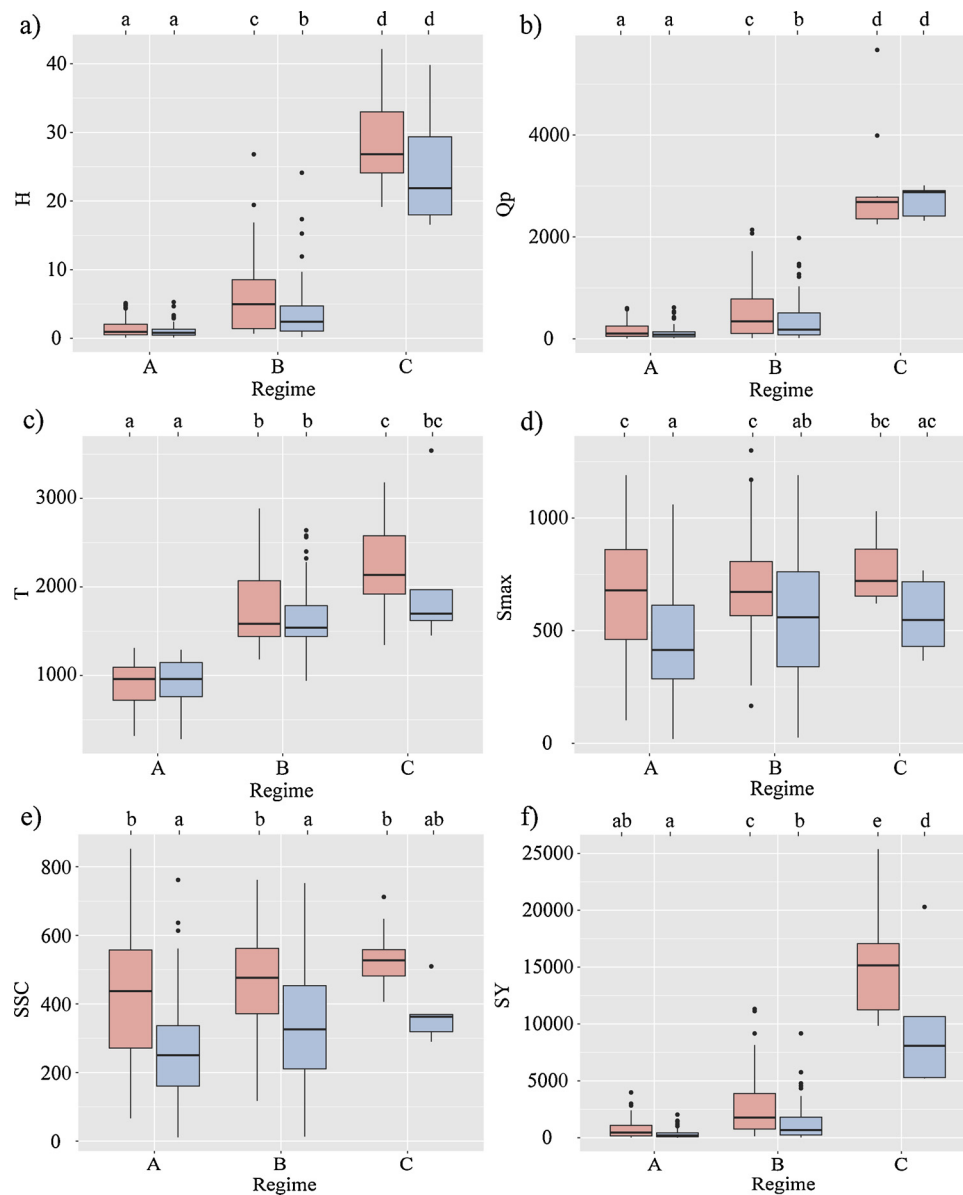


Fig. 3. Main Characteristics of the flood events in different period for different flood regimes (Note: The different letters at the top of each sub-figure indicate the differences are significant at $p < 0.01$ level; Red box plots represent the characteristics of hydrological variables in baseline period, and the blue box plot represents the characteristics of hydrological variables in changing period).

the summed sediment yield was 14.2 % (1.09×10^8 t), 51.8 % (3.99×10^8 t), and 34.0 % (2.62×10^8 t) for Regimes A, B, and C, respectively. In general, the flood events from Regime C contribute more than 30 % to total sediment yield with only ten flood events. This indicated that the major sediment-producing events mainly from Regime C. The runoff related variables (H and Q_p) presented large variability among different regimes. This may infer that the differences of different flood regimes in sediment yield were mainly runoff dependent.

4.3. Changes in runoff-sediment relationship

Fig. 4 shows the linear regression analysis between sediment yield and runoff depth for the all flood events in three regimes during the baseline period and changing period. The determination coefficients (R^2) were 0.89 and 0.87 for Regime B during the baseline period and changing period, respectively, and reached up to 0.96 for the Regime C during the two phases. However, it was relatively worse for the Regime

A which was dominated by small and medium flood runoff events. The result suggested that the variability of the runoff-sediment relationship remains relatively small. However, relatively lower coefficients ($R^2 = 0.83$ and $R^2 = 0.74$) were found for Regime A, which indicated that the relationship of $SY-H$ had great variability, and that the sediment yield by this regime could be regulated through the alteration of runoff-sediment relationships. In addition, the slope of regression equations could be considered to be representative of the sediment transport capacity per unit runoff depth. As shown in the Fig. 4, compared with the changing period, sediment transport capacity per unit runoff depth of the medium and small flood events (Regimes A and B) were obviously decreased during the changing period. However, the sediment transport capacity has changed little for the flood events of Regime C in the two phases.

4.4. Changes in hydrological variables influencing sediment yield

Stepwise multiple regressions were used to determine the major

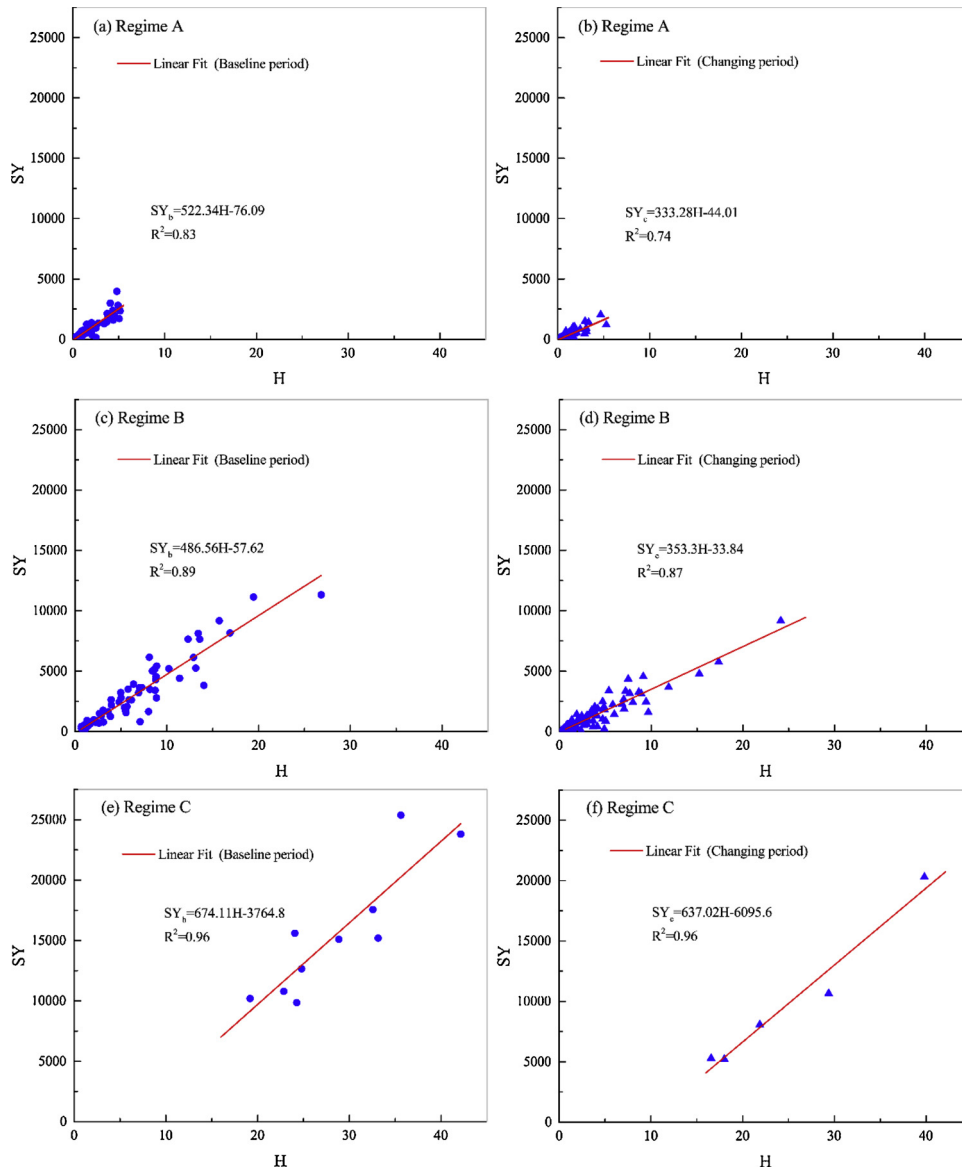


Fig. 4. Linear regression analysis between runoff depth (H) and sediment yield (SY) during the baseline period and changing period.

hydrological variables affecting suspended sediment yield for different flood regimes during the baseline period and changing period. Eqs. (9)–(11) showed the fundamental relationship formula between the dominant controlling variables and sediment yield for each flood regime during the baseline period:

$$SY = e^{3.06H^{0.59}Q_p^{0.62}}, R^2 = 0.882, P \leq 0.01(Regime_A) \quad (9)$$

$$SY = e^{4.42H^{0.67}Q_p^{0.37}}, R^2 = 0.911, P \leq 0.01(Regime_B) \quad (10)$$

$$SY = e^{1.09H^{1.37}T^{0.51}}, R^2 = 0.945, P \leq 0.01(Regime_C) \quad (11)$$

The Eqs. (12)–(14) are obtained for each flood regime during the changing period:

$$SY = e^{3.65H^{0.65}Q_p^{0.44}}, R^2 = 0.787, P \leq 0.01(Regime_A) \quad (12)$$

$$SY = e^{-0.04H^{0.53}Q_p^{0.58}T^{0.41}}, R^2 = 0.925, P \leq 0.01(Regime_B) \quad (13)$$

$$SY = e^{1.86H^{1.06}T^{0.51}}, R^2 = 0.994, P \leq 0.01(Regime_C) \quad (14)$$

According to Eqs. (8)–(13), the predominant hydrological variables (runoff depth, peak discharge, and flood duration) influencing suspended sediment yield varied with different flood regimes. The

sediment yield of small flood events (Regime A) were all mainly positively determined by runoff depth and peak discharge for the two period. However, the influence of peak discharge on sediment yield in the changing period was minor compared with that in the baseline period. No statistically significant correlation between flood duration and sediment yield was observed for this flood regime. In terms of medium flood events (Regime B), and the sediment yield had positive correlations with runoff depth and peak discharge in the baseline period, whereas the three runoff variables (H, Qp, and T) all play key roles in the sediment yield during the changing period. As for the large flood events (Regime C), sediment yield had a positive relationship with runoff depth and flood duration. Nevertheless, the sediment yield was immune to the impact of peak discharge for this regime in the two phases.

4.5. Event-based sediment yield prediction

The models were built using the support vector machine method. Fig. 5a, b, and c showed the comparison between observed and modeled sediment yield for the training set and test set. For Regime A, 120 flood events in training set were applied to train an SVM model, with a

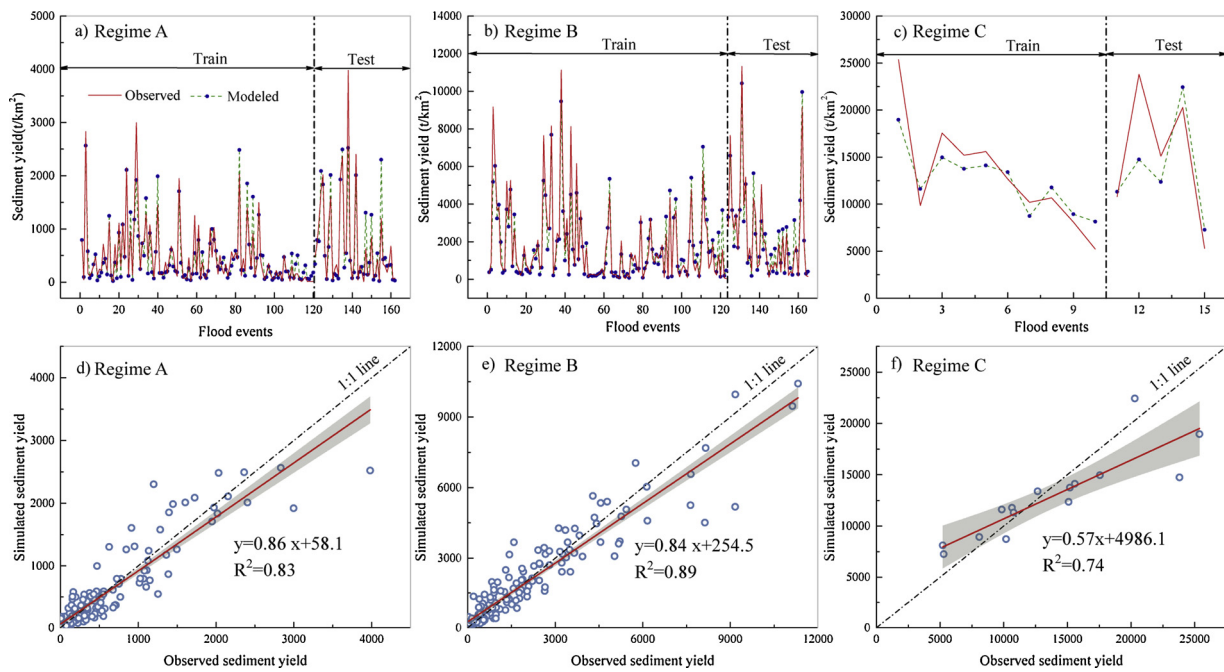


Fig. 5. Observed versus simulated sediment yield for different flood regime based on the SVM.

Table 2

The prediction performances of Support Vector Machine (SVM) Models.

Flood regime	Training process			Testing process		
	n	R ²	RMSE	n	R ²	RMSE
A	120	0.837	225.8	42	0.819	356.0
B	123	0.875	759.3	42	0.920	697.2
C	10	0.921	2613.0	5	0.595	4434.2

n: Number of flood events.

determination coefficient (R²) of 0.837 and an RMSE of 225.8 t/km² (Table 2). The remaining 42 events in the test set were used for testing the sediment yield model, whose R² and RMSE were 0.819 and 356.0 t/km². The relative high R² in both training process (R² = 0.875) and testing process (R² = 0.920) were detected for the Regime B. In terms of Regime C, the model performed well for the training set, with an R² of 0.921 and an RMSE of 166.65 t/km². Nevertheless, for the test set, the prediction result of the model was relatively poor (R² = 0.595). In addition, the relationships between observed and simulated sediment yield showed that the points mostly distributed around the 1:1 line (Fig. 5d, e, and f), indicating a good agreement between observed and simulated sediment load. Overall, according to the relationships between observed and simulated sediment yield (Fig. 5) and the prediction performances shown in Table 2, it is obvious that the performance of the models were relatively well for the various flood regimes. This indicated that the established models were capable of simulating the sediment yield of different flood regimes.

The residual error diagrams were used to further evaluate the performance of established models for different flood regimes (Fig. 6). The residual error is defined as observed sediment yield minus predicted sediment yield. As shown in Fig. 6, the overestimates (negative error) and underestimates (positive error) of sediment yield for events with different magnitudes many points could be identified in this plot. For the residuals of different flood regimes, a greater number of points were distributed around the line of y = 0, suggesting a relatively good prediction of sediment yield. However, for the Regime C, underestimates were made for most points of the high sediment yield events, whereas overestimated were observed for the low-magnitude sediment yield

events.

5. Discussion

5.1. Regime-based runoff and sediment characteristics

The present study categorizes a total of 342 flood events into three regimes. Flood regime A and B are characterized by a high frequency of flood events. However, the two flood regimes have only slight erosive effects on the soil and fail to cause the largest sediment yield. Only a small portion of the flood events belong to Flood Regime C, but yielding nearly the same amount of sediment load as those from flood Regime B, and three times that of flood Regime A. It indicated that a large proportion of sediment load resulted from a small number of flood events. This is consistent with previous studies in other agricultural watersheds (Estrany, Garcia, & Batalla, 2009; Lana-Renault & Regués, 2009; Mano, Nemery, Belleudy, & Poirel, 2009). Generally, many relatively minor floods contributed very limited sediment to the total sediment yield because of the low SY though the high occurrence frequency (Fig. 3). However, the contribution of these small-sediment-producing events to sediment delivery should not be ignored (Zheng, Cai, Chen, & Q.J., 2008). Large amounts of coarse sediment derived from splash erosion and scoured erosion might temporarily deposit in channel due to the low-magnitude flow transport capacity. The stored sediment would provide abundant sediment during the subsequent large-magnitude events.

Surface runoff acts as the primary medium for sediment transport. The correlation analysis indicates that the runoff depth displays a highest correlation with sediment yield (Fig. 2). And the runoff depth varies considerably across three flood regimes (Fig. 3). This finding confirms that sediment yield to a large extent is influenced by the runoff depth. Many previous studies also verified that runoff depth is a key factor in sediment detaching and delivering (Zheng & Chen, 2015; Zheng et al., 2012). However, relatively low correlation is observed between SSC and corresponding runoff variables (Fig. 2). This is mainly due to the frequently hyper-concentrated flow in the Loess plateau (Steege & Govers, 2010; Xu, 1999a), even when flow discharge was quite low. The sediment supply of Loess Plateau is generally abundant without limit and rainfall usually occurs as high-intensity storm of short

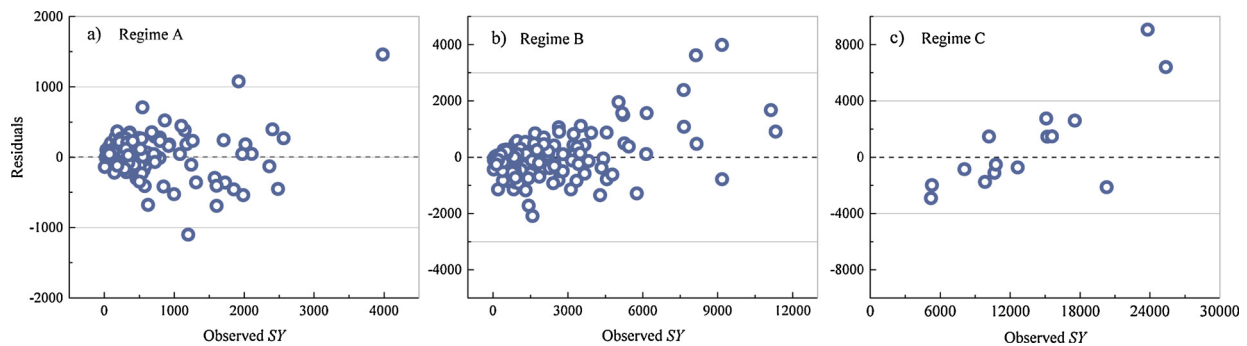


Fig. 6. The residual error between predicted and observed sediment yield.

duration, which is prone to produce hyper-concentrated flow (Xu, 2004; Zheng et al., 2012). Especially in the Gushanchuan catchment, a typical coarse sand source catchment, the SSC depended largely on the transport capacity of surface runoff instead of runoff volume (i.e. small flood events could generate hyper-concentrated flow). This can be further verified in the current study, where the difference between the SSC of three flood regimes is not significant though the differences are significant in runoff depth (Fig. 3). The poor SSC-Q statistical relationship was consistent with other researches of event-related suspended sediment dynamics (Estrany et al., 2009; Pierson, 2005). As Zheng et al. (2012) confirmed, SSC had no correlation with H at various spatial scales from hillslope to river channel for a single event. Therefore, the differences in SSC have limited effects on the variation of the sediment yield for three flood regimes.

Numerous previous studies have focused on investigating the relationships between the runoff and event sediment yield using correlation analyses (Cai, Liu, & Liu, 2004; Lane, Hernandez, & Nichols, 1997). In the loess areas, a good agreement between event sediment yield and event runoff volume has been detected for linear regression models (Wang & Zhang, 1990) and power regression models (Mou & Meng, 1981), and the determination coefficients were usually more than 0.9. Additionally, Zheng et al. (2008) found that linear equations ($y = ax + b$) could explain the observed variance better than power equations ($y = ax^b$) for 12 small watersheds in hilly areas of the Loess Plateau. Especially for high-magnitude events, the linear equation offer far greater performance. However, just as the result in this study, the linear equations have the disadvantage for low runoff depth. The negative sediment yield will be obtained for low flow and zero flow from these equations (Fig. 4). Nevertheless, for the large flood event (Regime C), the negative intercept values do not have an influence on the predicted sediment yield because the runoff depth of these flood events exceed 15 mm (Fig. 4e and f).

5.2. Influence of sediment control measures on runoff-sediment relationships of different flood regimes

The runoff-sediment relationship is critical to understand soil erosion and sediment yield in severe eroded areas. Previous research has identified a dramatic effect of soil and water conservation measures on this relationship (Braud, Vich, Zuluaga, Fornero, & Pedrani, 2001; Zheng et al., 2012). As Liang et al. (2015) reported, the soil and water conservation measures in the Loess Plateau mainly include biological and engineering measures, which could change local microtopography, intercept precipitation, increase flow infiltration rate, delay or retain runoff, and can reduce rainfall energy on soil erosion and sediment transport capacity. These different measures thus may greatly impact the temporal and spatial distribution of runoff and sediment flow.

In the past several decades, a series of soil and water conservation measures (including terraces, check-dams, and vegetation measures) have been implemented to control the soil erosion. Vegetation measures focus on controlling soil erosion on hillslopes, while they fail to reduce

the gravity erosion and gully erosion effectively. However, the gully density is extremely large in the highly erodible catchments of the Loess Plateau. The sediment of these catchments was mainly supplied by gully, bank, and channel erosion (the sediment deposited in the river bed and channel prior to flood event). Since the vegetation can change the topographic characteristics of gullies and channels, thus, for meso-scale and large scale catchments in the Loess Plateau, the impact of vegetation and other soil and water conservation measures of hillslopes on sediment reduction is mainly realized by decreasing runoff volume. Zheng et al. (2007) assessed the vegetation effects on runoff-sediment yield relationship at various spatial scales, and confirmed that it is much more difficult to change the relationship between runoff and sediment at the watershed scale. By contrast, the check-dams constructed in gullies or channels are expected to trap most of the incoming sediment from the upstream (Boix-Fayos, Barberá, López-Bermúdez, & Castillo, 2007; Cerda, 1998). The check-dams could uplift the base-level and decrease the gradient of gullies, which then completely alters surface hydrology as well as sediment deposition and reduces runoff erosivity and sediment-carrying capacity of runoff (Xu, 1999b).

Numerous studies have confirmed that soil and water conservation measures played an indispensable role in the reduction of runoff and sediment load (Rustomji, Zhang, Hairsine, Zhang, & Zhao, 2008; Zhao et al., 2016). However, there might be differences in the mechanism of sediment reduction for different flood regimes. Zheng et al. (2008) and Zheng et al. (2013) found out that the runoff-sediment relationship almost does not change with the implementation of human-dominated vegetation restoration measures for large runoff events, which is consistent with the results of this study (Fig. 4e and f). Consequently, for Regime C, the variations of sediment yield primary result from the differences in flood runoff amount before and after the implementation of soil and water conservation measures. Nevertheless, for the minor flood events (Regimes A and B), the runoff-sediment relationship might be unsteady. The runoff-sediment relationships will be inevitably changed due to the implementation of soil and water conservation measures. Accordingly, the changes in sediment yield for Regimes A and B is partly regulated by altering of runoff-sediment relationships. Therefore, figuring out the mechanism of sediment reduction will be beneficial to assess the effectiveness of soil and water conservation measures.

6. Conclusion

A total of 342 events from 1954 to 2015 were selected to assess the effects of conservation measures on runoff-sediment relationships under different flood regimes in the Gushanchuan catchment from the Loess Plateau. Three flood regimes were classified using hierarchical clustering method based on runoff depth, flood duration, and peak discharge. The following conclusions can be drawn from our study.

The main characteristics (H , Q_p , SY , S_{max} , and SSC) of flood events experienced reductions for all flood regimes during the baseline period compared with those in changing period the of the flood events. For the

three flood regimes, Regime C was characterized by its low frequency and the highest sediment yield amount at a single event scale. Linear regression analysis between runoff depth and suspended sediment yield showed that the runoff-sediment relationship remains relatively constant for large flood regimes (Regime C), while the relationship was variable for relatively minor flood events (Regimes A and B). Additionally, the performance of fitting equations for runoff indices and sediment yield was rather poor for the flood events in the changing period. Event sediment yield of Regime C was positively correlated with runoff depth and peak discharge. For Regime A, sediment yield were all mainly positively determined by runoff depth and peak discharge for the two periods. As for Regime B, sediment yield has strong positive correlations with runoff depth and peak discharge in the baseline period, whereas the three runoff variables (H , Q_p , and T) all play key roles in the sediment yield during the changing period. The models established by SVM were used to simulate the event-based sediment yield, and the correspondence between the observed and simulated sediment yield was examined. The simulation results indicated that these models are capable of predicting the sediment yield of different flood regimes with relatively high precision.

Declaration of Competing Interest

We declare that we have no conflict of interest.

Acknowledgements

The work was funded by the National Key Scientific Research Project (2016YFC0402401), National Natural Science Foundation of China (41671285; 51509206), the Shaanxi Youth Science and Technology Star Project (2015KJXX-58), and Special-Funds of Scientific Research Programs of State Key Laboratory of Soil Erosion and Dryland Farming on the Loess Plateau (A314021403-Q2). We also thank the National Climatic Centre and the Hydrology Bureau of the Yellow River Water Resources Commission for providing valuable climatic and hydrological data. The authors would also thank for the very valuable comments from reviewers which greatly improved the quality of the paper.

References

- Bautista, S., Mayor, A. G., Bourakhouadar, J., & Bellot, J. (2007). Plant spatial pattern predicts hillslope runoff and erosion in a semi-arid mediterranean landscape. *Ecosystems*, *10*, 987–998.
- Boix-Fayos, C., Martínez-Mena, M., Arnau-Rosalén, E., Calvo-Cases, A., Castillo, V., & Albaladejo, J. (2006). Measuring soil erosion by field plots: Understanding the sources of variation. *Earth-Science Reviews*, *78*, 267–285.
- Boix-Fayos, C., Barberá, G. G., López-Bermúdez, F., & Castillo, V. M. (2007). Effects of check dams, reforestation and land-use changes on river channel morphology: Case study of the rogativa catchment (Murcia, Spain). *Geomorphology*, *91*, 103–123.
- Braud, I., Vich, A. I. J., Zuluaga, J., Fornero, L., & Pedrani, A. (2001). Vegetation influence on runoff and sediment yield in the Andes region: Observation and modelling. *Journal of Hydrology*, *254*, 124–144.
- Buendia, C., Bussi, G., Tuset, J., Vericat, D., Sabater, S., Palau, A., et al. (2016). Effects of afforestation on runoff and sediment load in an upland Mediterranean catchment. *The Science of the Total Environment*, *540*, 144–157.
- Cai, Q. G., Liu, J. G., & Liu, Q. J. (2004). Research of sediment yield statistical model for singlerainstorm in Chabagou drainage basin. *Geographical Research*, *23*, 433–439 (in Chinese).
- Cerda, A. (1998). The influence of geomorphological position and vegetation cover on the erosional and hydrological processes on a Mediterranean hillslope. *Hydrological Processes*, *12*, 661–671.
- Chang, C. C., & Lin, C. J. (2011). LIBSVM: A library for support vector machines. *ACM Transactions on Intelligent Systems and Technology*, *2(27)* 1–27:27. Software available at <http://www.csie.ntu.edu.tw/~cjlin/libsvm>.
- Chaplot, V., & Poesen, J. (2012). Sediment, soil organic carbon and runoff delivery at various spatial scales. *Catena*, *88*, 46–56.
- El Kateb, H., Zhang, H. F., Zhang, P. C., & Mosandl, R. (2013). Soil erosion and surface runoff on different vegetation covers and slope gradients: A field experiment in Southern Shaanxi Province, China. *Catena*, *105*, 1–10.
- Estrany, J., Garcia, C., & Batalla, R. J. (2009). Suspended sediment transport in a small Mediterranean agricultural catchment. *Earth Surface Processes and Landforms*, *34*, 929–940.
- Fang, H. Y., Cai, Q. G., Chen, H., & Li, Q. Y. (2008). Effect of rainfall regime and slope on runoff in a gullied loess region on the Loess Plateau in China. *Environmental Management*, *42*, 402–411.
- Fang, N. F., Shi, Z. H., Li, L., Guo, Z. L., Liu, Q. J., & Ai, L. (2012). The effects of rainfall regimes and land use changes on runoff and soil loss in a small mountainous watershed. *Catena*, *99*, 1–8.
- Gain, A. K., & Wada, Y. (2014). Assessment of future water scarcity at different spatial and temporal scales of the Brahmaputra River Basin. *Water Resources Management*, *28*, 999–1012.
- Gao, G. Y., Ma, Y., & Fu, B. J. (2016). Temporal variations of flow-sediment relationships in a highly erodible catchment of the Loess Plateau, China. *Land Degradation & Development*, *27*, 758–772.
- Lal, R. (2003). Soil erosion and the global carbon budget. *Environment International*, *29*, 437–450.
- Lana-Renault, N., & Regüés, D. (2009). Seasonal patterns of suspended sediment transport in an abandoned farmland catchment in the Central Spanish Pyrenees. *Earth Surface Processes and Landforms*, *34*, 1291–1301.
- Lane, L. J., Hernandez, M., & Nichols, M. (1997). Processes controlling sediment yield from watersheds as functions of spatial scale. *Environmental Modelling & Software*, *12*, 355–369.
- Li, P. F., Mu, X. M., Holden, J., Wu, Y. P., Irvine, B., Wang, F., et al. (2017). Comparison of soil erosion models used to study the Chinese Loess Plateau. *Earth-Science Reviews*, *170*, 17–30.
- Liang, W., Bai, D., Wang, F. Y., Fu, B. J., Yan, J. P., Wang, S., et al. (2015). Quantifying the impacts of climate change and ecological restoration on streamflow changes based on a Budyko hydrological model in China's Loess Plateau. *Water Resources Research*, *51*, 6500–6519.
- Lørup, J. K., Refsgaard, J. C., & Mazvimavi, D. (1998). Assessing the effect of land use change on catchment runoff by combined use of statistical tests and hydrological modelling: Case studies from Zimbabwe. *Journal of Hydrology*, *205*, 147–163.
- Lu, H., Moran, C. J., & Sivapalan, M. (2005). A theoretical exploration of catchment-scale sediment delivery. *Water Resources Research*, *41*, W09415.
- Mano, V., Nemery, J., Belleudy, P., & Poirel, A. (2009). Assessment of suspended sediment transport in four alpine watersheds (France): Influence of the climatic regime. *Hydrological Processes*, *23*, 777–792.
- Mou, J. Z., & Meng, Q. M. (1981). Annual sediment yield calculation of small and large watersheds in the north of Shaanxi Province. In Institute of Soil and Water Conservation, Chinese Academy of Science (Ed.). *Research on soil conservation practice on Loess Plateau, Beijing* (pp. 251–255). (in Chinese).
- Mu, X. M., Zhang, L., McVicar, T. R., Chille, B., & Gao, P. (2007). Analysis of the impact of conservation measures on stream flow regime in catchments of the Loess Plateau, China. *Hydrological Processes*, *21*, 2124–2134.
- Mullan, D. (2013). Managing soil erosion in Northern Ireland: A review of past and present approaches. *Agriculture*, *3*, 684–699.
- Parsons, A. J., & Stone, P. M. (2006). Effects of intra-storm variations in rainfall intensity on interrill runoff and erosion. *Catena*, *67*, 68–78.
- Peng, T., & Wang, S. J. (2012). Effects of land use, land cover and rainfall regimes on the surface runoff and soil loss on karst slopes in southwest China. *Catena*, *90*, 53–62.
- Pierson, T. C. (2005). *Hyperconcentrated flow—Transitional process between water flow and debris flow, Debris-flow hazards and related phenomena*. Springer159–202.
- Pimentel, D. (2006). Soil erosion: A food and environmental threat. *Environment, Development and Sustainability*, *8*, 119–137.
- Ran, Q. H., Su, D. Y., Li, P., & He, Z. G. (2012). Experimental study of the impact of rainfall characteristics on runoff generation and soil erosion. *Journal of Hydrology*, *424–425*, 99–111.
- Robinson, D. A., & Blackman, J. D. (1990). Soil erosion and flooding: Consequences on land use policy and agricultural practice on the South Downs, East Sussex, UK. *Land Use Policy*, *7*, 41–52.
- Rustomji, P., Zhang, X. P., Hairsine, P. B., Zhang, L., & Zhao, J. (2008). River sediment load and concentration responses to changes in hydrology and catchment management in the Loess Plateau region of China. *Water Resources Research*, *44*, W00A04.
- Shi, H. Y., & Wang, G. Q. (2015). Impacts of climate change and hydraulic structures on runoff and sediment discharge in the middle Yellow River. *Hydrological Processes*, *29*, 3236–3246.
- Simonneaux, V., Cheggour, A., Deschamps, C., Mouillot, F., Cerdan, O., & Le Bissonnais, Y. (2015). Land use and climate change effects on soil erosion in a semi-arid mountainous watershed (High Atlas, Morocco). *Journal of Arid Environments*, *122*, 64–75.
- Steenen, A., & Govers, G. (2010). Correction factors for estimating suspended sediment export from loess catchments. *Earth Surface Processes and Landforms*, *26*, 441–449.
- Tian, P., Zhai, J. Q., Zhao, G. J., & Mu, X. M. (2016). Dynamics of runoff and suspended sediment transport in a highly erodible catchment on the Chinese Loess Plateau. *Land Degradation and Development*, *27*, 839–850.
- Verstraeten, G., & Poesen, J. (2001). Factors controlling sediment yield from small intensively cultivated catchments in a temperate humid climate. *Geomorphology*, *40*, 123–144.
- Verstraeten, G., Prosser, I. P., & Fogarty, I. P. (2007). Predicting the spatial patterns of hillslope sediment delivery to river channels in the Murrumbidgee catchment, Australia. *Journal of Hydrology*, *334*, 440–454.
- Walling, D. E. (1999). Linking land use, erosion and sediment yields in river basins. *Hydrobiologia*, *410*, 223–240.
- Walling, D. E. (2006). Human impact on land-ocean sediment transfer by the world's rivers. *Geomorphology*, *79*, 192–216.
- Wang, H., Yang, Z. S., Saito, Y., Liu, J. P., Sun, X. X., & Wang, Y. (2007). Stepwise decreases of the Huanghe (Yellow River) sediment load (1950–2005): Impacts of climate change and human activities. *Global and Planetary Change*, *57*, 331–354.

- Wang, M. L., & Zhang, R. (1990). Study on sediment yield model under single storm in Chabagou watershed. *Journal of Soil and Water Conservation*, 4, 11–18 (in Chinese).
- Wasson, R. J. (1994). Annual and decadal variation of sediment yield in Australia, and some global comparisons. *IAHS Publication*, 224, 269–279.
- Wu, J. W., Miao, C. Y., Zhang, X. M., Yang, T. T., & Duan, Q. Y. (2017). Detecting the quantitative hydrological response to changes in climate and human activities. *The Science of the Total Environment*, 586, 328–337.
- Xu, J. X. (1999a). Erosion caused by hyperconcentrated flow on the Loess Plateau of China. *Catena*, 36, 1–19.
- Xu, J. X. (1999b). Physico-geographical factors for the formation of hyperconcentrated flows in the Loess Plateau of China. *Acta Geographica Sinica*, 54, 318–326 (In Chinese).
- Xu, J. X. (2004). Hyperconcentrated flows in the slope-channel systems in gullied hilly areas on the loess plateau, China. *Geografiska Annaler Series A*, 86A, 349–366.
- Yang, T., Xu, C. Y., Chen, X., Singh, V. P., Shao, Q. X., Hao, Z. C., et al. (2010). Assessing the impact of human activities on hydrological and sediment changes (1953–2000) in nine major catchments of the Loess Plateau. *River Research and Applications*, 26, 322–340.
- Yellow River Conservancy Committee (2015). *Hydrological year book of the Yellow River*. Yellow River Conservancy Press.
- Yue, X. L., Mu, X. M., Zhao, G. J., Shao, H. B., & Gao, P. (2014). Dynamic changes of sediment load in the middle reaches of the Yellow River basin, China and implications for eco-restoration. *Ecological Engineering*, 73, 64–72.
- Zhang, L. T., Li, Z. B., Wang, H., & Xiao, J. B. (2016). Influence of intra-event-based flood regime on sediment flow behavior from a typical agro-catchment of the Chinese loess plateau. *Journal of Hydrology*, 538, 71–81.
- Zhang, X. C., & Liu, W. Z. (2005). Simulating potential response of hydrology, soil erosion, and crop productivity to climate change in Changwu tableland region on the Loess Plateau of China. *Agricultural and Forest Meteorology*, 131, 127–142.
- Zhao, G. J., Kondolf, G. M., Mu, X. M., Han, M. W., He, Z., Rubin, Z., et al. (2016). Sediment yield reduction associated with land use changes and check dams in a catchment of the Loess Plateau, China. *Catena*, 148, 126–137.
- Zhao, G. J., Yue, X. L., Tian, P., Mu, X. M., Xu, W. L., Wang, F., et al. (2017). Comparison of the Suspended Sediment Dynamics in Two Loess Plateau Catchments, China. *Land degradation and Development*, 28, 1398–1411.
- Zhao, G. J., Mu, X. M., Jiao, J. Y., Xu, W. L., Wang, F., Gao, P., et al. (2018). Assessing response of sediment load variation to climate change and human activities with six different approaches. *The Science of the Total Environment*, 639, 773–784.
- Zheng, M. G., & Chen, X. A. (2015). Statistical determination of rainfall-runoff erosivity indices for single storms in the Chinese Loess Plateau. *PLoS One*, 10, e0117989.
- Zheng, M. G., Cai, Q. G., & Chen, H. (2007). Effect of vegetation on runoff-sediment yield relationship at different spatial scales in hilly areas of the Loess Plateau, North China. *Acta Ecologica Sinica*, 27, 3572–3581.
- Zheng, M. G., Cai, Q. G., Chen, G., & Q. J. (2008). Modelling the runoff-sediment yield relationship using a proportional function in hilly areas of the Loess Plateau, North China. *Geomorphology*, 93, 288–301.
- Zheng, M. G., Yang, J. S., Qi, D. L., Sun, L. Y., & Cai, Q. G. (2012). Flow-sediment relationship as functions of spatial and temporal scales in hilly areas of the Chinese Loess Plateau. *Catena*, 98, 29–40.
- Zheng, M. G., Qin, F., Yang, J. S., & Cai, Q. G. (2013). The spatio-temporal invariability of sediment concentration and the flow-sediment relationship for hilly areas of the Chinese Loess Plateau. *Catena*, 109, 164–176.